^{56}Fe(e,α) reaction and its relevance to the $E2$ isoscalar sum rule

D. M. Skopik, J. Asai, and J. J. Murphy II
Saskatchewan Accelerator Laboratory, University of Saskatchewan, Saskatoon S7N 0W0, Canada
(Received 17 December 1979)

The cross section ^{56}Fe(e,α) has been measured as a function of α energy, lab angle, and incident electron energy. The analyses of these data using distorted-wave Born approximation virtual photon spectra have been performed in the framework of models suggested by the data. We find that the (e,α) channel exhausts a sizable percentage of the $E2$ isoscalar sum rule.

[NUCLEAR REACTIONS ^{56}Fe(e,α) measured $\sigma(E_0, E_\alpha, \theta_\alpha)$, obtained $\sigma(e,\alpha)$ and determined $\sigma^{E1}(\gamma,\alpha)$ and $\sigma^{E2}(\gamma,\alpha)$.]

I. INTRODUCTION

The work that we report here is an outgrowth of our earlier (e,α) experiments[1,2] in which the systematics of alpha emission from various nuclei after electron bombardment were studied. The primary motivation for this experiment, however, was the recent work by Wolynec *et al.*[3] in which it was concluded that the $E2$ isoscalar resonance for ^{58,60,62}Ni decays predominantly through the alpha channel. They reported that roughly 30–50% of the $E2$ sum rule was exhausted by the (γ,α) reaction, and while this percentage exhaustion has been lowered after reanalysis,[4] the conclusion is still that the (γ,α) channel is a dominant decay mode of the $E2$ isoscalar resonance for these nuclei.

We have measured the ^{56}Fe(e,α) cross section to see if a similar effect exists in this nucleus. As was the case in ^{60}Ni, the capture reaction ^{52}Cr$(\alpha,\gamma_0)^{56}$Fe is small and the amount of $E2$ strength located near 16 MeV (60 $A^{-1/3}$) is less than 1%.[5] Hence the picture proposed by Wolynec *et al.* that the α's preferentially decay not to the ground state but rather to the first excited state in ^{52}Cr by s, d, or g waves may also be applicable in ^{56}Fe (see Fig. 1).

The technique that the National Bureau of Standards group used was to measure yields of the (e,α) cross section and then use a modified Lorentzian line shape to unfold the $E1$ and $E2$ cross sections. Subsequent analysis has shown that the $E1$ analysis is independent of an assumed line shape.[4] The indicator in their work that $E2$ transitions are an important factor is the rapid rise of the yield as the incident energy increases. This is due to the fact that the number of $E2$ virtual photons is greater than the number of $E1$ photons. If only $E1$ transitions were important, the slope of the isochromat would be much less, as is demonstrated by their (e,p) measurement which proceeds essentially by $E1$ processes. The point has been raised by the Glasgow group[6] that the increase in the isochromat as E_0 increases may be accounted for by a statistical model. We can fit our measured energy distributions with a statistical model that gives reasonable parameters (e.g., nuclear temperatures of ~0.3 MeV). Because of this we have looked as well at the angular dependence of the emitted α particles, since a statistical interpretation of data such as these would demand that the angular distribution be symmetric about 90°, whereas if direct or reso-

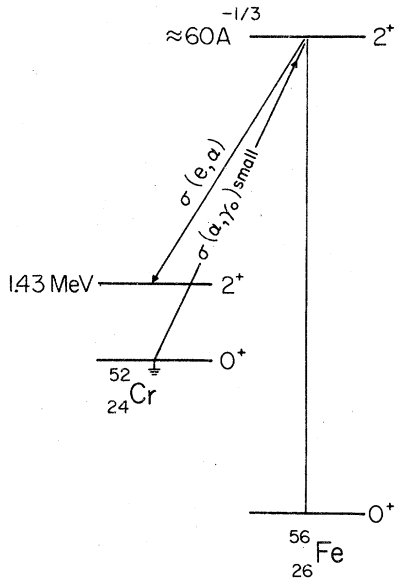

FIG. 1. $E2$ decay scheme for the ^{56}Fe(e,α) reaction, equivalent to the one proposed for ^{58}Ni by Wolynec *et al.* (Ref. 3). The ground state channel, as noted in the diagram is small (Ref. 5).

nance effects are present the angular distributions may be asymmetric.[7]

II. EXPERIMENTAL PROCEDURE

The apparatus used in this experiment was similar to the one used in our earlier work.[1,2] The α particles were detected by a positive-ion spectrometer which consisted of five silicon surface barrier detectors positioned in the focal plane of a 127° double-focusing magnet. The beam current was measured by a nonintercepting ferrite monitor that was periodically calibrated with a Faraday cup.

The iron foils used in this experiment were 2.0 and 3.9 mg/cm^2. The thicknesses of the foils were determined by both direct micrometer measurement and by measuring the energy loss of 5.49 MeV α particles in passing through the foils.

The overall experimental uncertainty, reflecting errors in measuring the incident charge, target thickness, solid angle, and detector efficiencies, is ± 5%.

As well as electrodisintegration data, photodisintegration data were also taken by inserting a thin (22 mg/cm^2) Ta radiator in front of the target. Checks were made by varying the thickness of the radiator to ensure that a thin enough radiator was used, which allowed us to ignore thick target effects. The position of the radiator along the incident beam line was found not to affect the count rate of α particles in the spectrometer.

The radiator data were taken only to ascertain that we are justified in neglecting $E\emptyset$ continuum contributions to the (e,α) cross section. The $E\emptyset$ isoscalar resonance, located at $\sim 80A^{-1/3}$ MeV, is not expected to contribute at the excitation energies that we are predominantly measuring $E_x \lesssim 20$ MeV.

III. RESULTS

A. Energy spectra

The (e,α) cross section as a function of α energy was measured at a number of incident electron energies. The spectra at 35 and 100 MeV are shown in Fig. 2. The 100 MeV run was performed to add to the systematics that were studied in our earlier work. Since the virtual photon theories currently available do not include corrections for finite size effects the incident energy was kept at $E_0 \lesssim 50$ MeV for the main body of the experimental data. Above 60 MeV the point nucleus approximation made in deriving the virtual photon spectra is not valid.[8]

For cross sections as a function of α-particle energy we can use a statistical or evaporation interpretation of the (e,α) process to fit the data. These fits, shown in Fig. 2 by the solid lines, give nuclear temperatures of 0.3 MeV. However, the nuclear temperature is essentially determined by the Coulomb barrier and the penetrability, i.e., it is determined primarily by where the cross section peaks. These energy distributions are similar to those that we have measured for other nuclei. The value of 0.3 MeV for ^{56}Fe is not inconsistent with the systematics deduced from our other data.

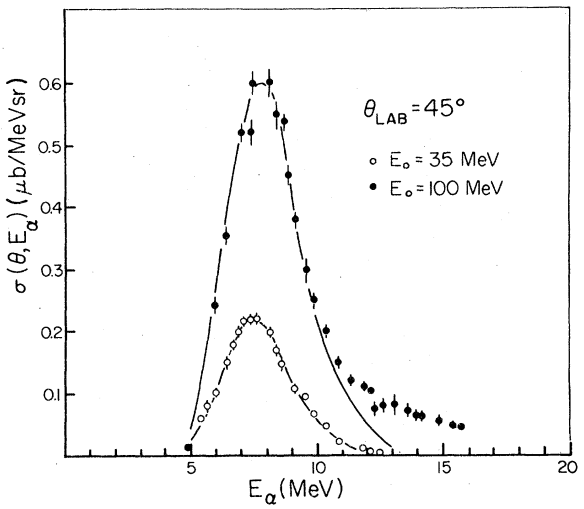

FIG. 2. Measured differential cross sections at θ_{LAB} = 45° for incident electron energies of 35 and 100 MeV. The solid lines are fits using the statistical model employed in our earlier studies of the (e,α) reaction from various nuclei. These fits result in a nuclear temperature of 0.3 MeV.

B. Angular distribution

If a statistical model analysis of the data is adopted, then the angular distribution of α particles is expected to be symmetric about 90°. We have measured a six point angular distribution for $E_0 = 35$ MeV over a wide range of α-particle energies. Representative angular distribution data are shown in Fig. 3. The data have been analyzed by fitting to the form

$$\sigma(\theta, E) = a + b\sin^2\theta + c\sin^2\theta\cos\theta + d\sin^2\theta\cos^2\theta . \quad (1)$$

In this form of fitting, the coefficient "c" arises from interference of opposite parity transitions. A finite value of c would not be explained by a statistical picture of the (e,α) process. The results of fitting the angular distribution data are shown in Fig. 4 and as can be seen, a finite value

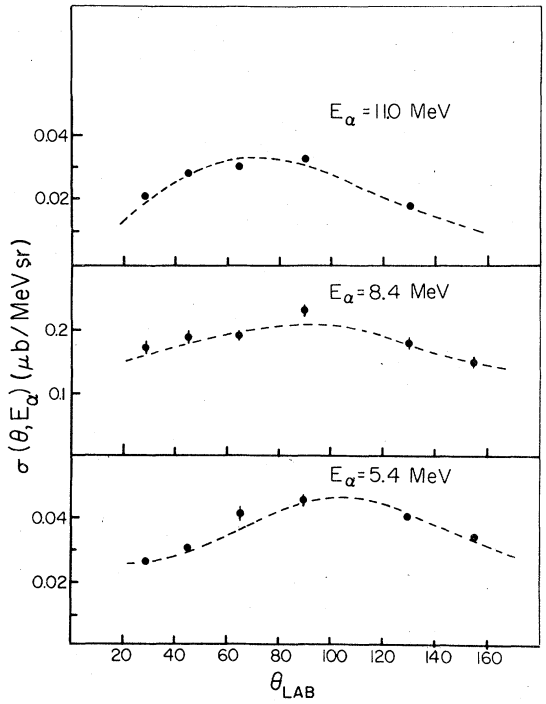

FIG. 3. Representative angular distributions that show the shift from backward to forward angles of α particles.

of the asymmetry, defined as $\beta = c/b$, is observed. A model-dependent explanation of the energy dependence of the asymmetry will be given in the next section.

The value of "d" was found to be consistent with zero over the range of α particles measured. This implies that d-wave emission of α particles is small. This result is consistent with the (α, γ_0) measurement since the decay to the ground state involves d-wave emission (recall that the capture results indicate a very small cross section) while decay to the 2^+ first excited state would involve primarily s-wave emission due to angular momentum arguments. As can be seen from the angular distribution data, a sizable isotropic term is measured, in marked contrast to the case when one restricts the α's to be emitted to the ground state, i.e., the capture results, where "a" is identically zero.

C. Isochromat data

At fixed α energies, the incident electron energy was varied from 26 to 50 MeV. Representative integrated over angle data are shown in Fig. 5, corresponding to an α energy near the peak in the energy distribution that is shown in Fig. 2. The analysis of these data will be explained in the next section.

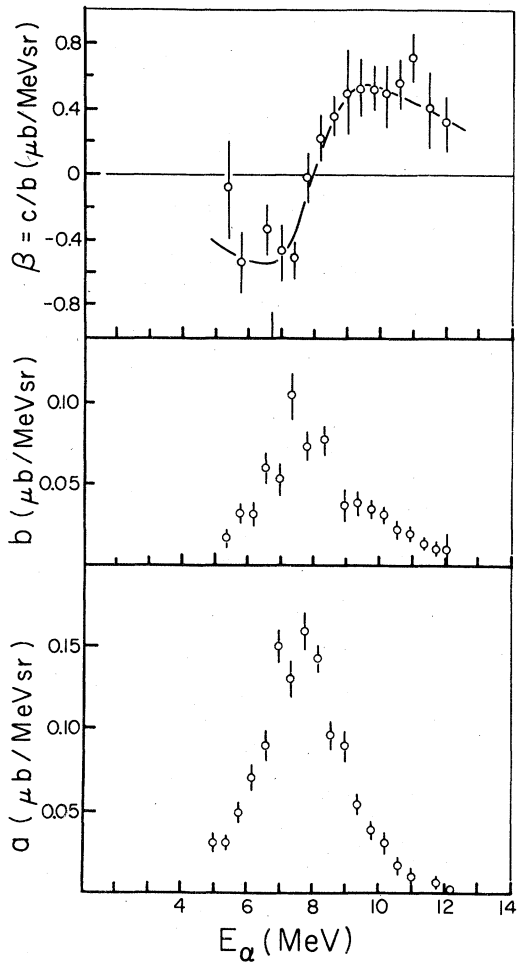

FIG. 4. Angular distribution coefficients (μb/MeV sr) that are found by fitting to Eq. (1). The asymmetry $\beta = c/b$ shows a change in sign that can be associated with resonance interference. The solid line is the result of fitting to an asymmetry defined in the text.

IV. MODEL-DEPENDENT ANALYSES

A. Angular distribution data

To account for the energy dependence of the asymmetry in the angular distribution data, we assume that the transition matrix element can be written in the usual notation as being proportional to

$$\left\langle \phi_f \left| r Y_{10} + \frac{f(r)}{E - E_R + \frac{1}{2} i\Gamma} Y_{20} \right| \Phi_i \right\rangle ,$$

which leads to an asymmetry:

$$\beta = F_1 \left[\frac{(E - E_R)}{(E - E_R)^2 + \Gamma^2/4} \right] - F_2 \left[\frac{\Gamma}{(E - E_R)^2 + \Gamma^2/4} \right] .$$

The quantities F_1 and F_2 are determined by least squares fitting and are related to the $E1$ and $E2$

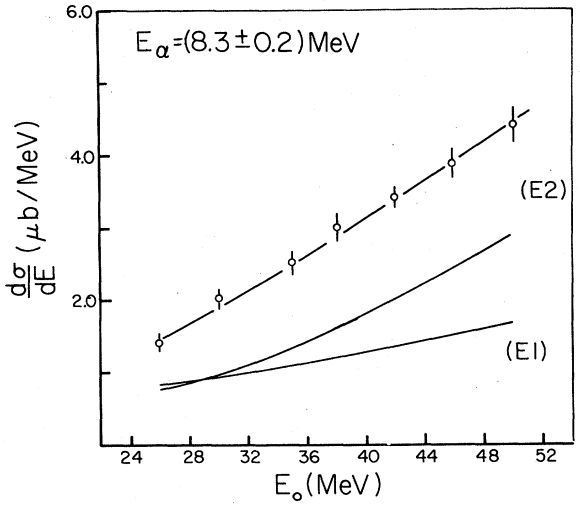

FIG. 5. The cross section $d\sigma/dE$ found by integrating over $d\Omega$ using the angular dependence shown in Fig. 4. These data are analyzed in terms of α particles making transitions to the 2^+ state in ^{52}Cr. The solid lines are the contributions to the cross section from $E1$ and $E2$ cross sections by least squares fitting Eq. (3).

matrix elements. All we are interested in here is to ascertain if the energy dependence of β can be explained by this simple model which contains resonance and direct interference terms.

The best fit to the data is shown by the solid line in Fig. 4. The resonance parameters determined are

$$\Gamma = 3.1 \pm 1.6 \text{ MeV},$$

$$E_R = 17.6 \pm 0.9 \text{ MeV } (8.0 \pm 0.4 \text{ MeV } \alpha \text{ energy}).$$

Again, we point out that statistical processes involve symmetric distributions ($\beta = 0$) and direct processes alone cannot account for the change of sign in β.

B. Isochromat analysis

Since the angular distribution exhibits a definite asymmetry about 90°, we have analyzed our data assuming that the α particles are making transitions to the 2^+ first excited state in ^{52}Cr. In other words, we adopt the decay scheme that is shown in Fig. 1. We further assume that only $E1$ and $E2$ multipoles contribute to the cross section. The results of our real photon measurements that are discussed later rule out any significant contribution to the cross section from $E\emptyset$ transitions which are allowed in the electrodisintegration process but not in photodisintegration.

In general, the total electrodisintegration cross section can be expressed as

$$\sigma_{e,\alpha}(E_0) = \sum_l \int_{E_t}^{E_0} \sigma_{\gamma,\alpha}^{(l)} N^{(l)}(E_0, E_\gamma Z) \frac{dE_\gamma}{E_\gamma}, \quad (2)$$

where the sum over l encompasses all multipoles, and E_t is the threshold for the reaction.

The quantity $N^l(E_0, E_\gamma, Z)$ has been computed by Wright.[9] The distortion for the $E1$ and $E2$ spectrum defined as the distorted wave to plane wave ratio is shown in Figs. 6 and 7, respectively. These distortions were used to calculate the photon spectra in all the following analyses.

In charged particle experiments, a total cross section is seldom measured. The total cross section is defined as

$$\sigma_{e,\alpha}(E_0) = \int_0^{E_{\alpha\max}} \frac{d^2\sigma}{d\Omega\, dE}\, d\Omega\, dE,$$

where the experimentally determined quantity is $d^2\sigma/d\Omega\, dE$. Therefore, assuming that the α particles are primarily emitted to the 2^+ excited state in ^{52}Cr, the integral in Eq. (2) can be evaluated at fixed gamma ray energies, if the angular dependence is removed. The angular dependence was determined from the coefficients of the fit to the angular distribution data given by Eq. (1), evaluated at 45°, the angle at which the energy dependence was studied. These coefficients were assumed to be independent of the incident electron energy in this analysis. Thus we form the cross sections (isochromats)

$$\frac{d\sigma}{dE} = \sigma_{\gamma,\alpha}^{E1}(E_\gamma) \frac{N^{E1}(E_0, E_\gamma, Z)}{E_\gamma} + \sigma_{\gamma,\alpha}^{E2}(E_\gamma) \frac{N^{E2}(E_0, E_\gamma, Z)}{E_\gamma}. \quad (3)$$

These cross sections were then fitted by minimizing χ^2, which determined the quantities

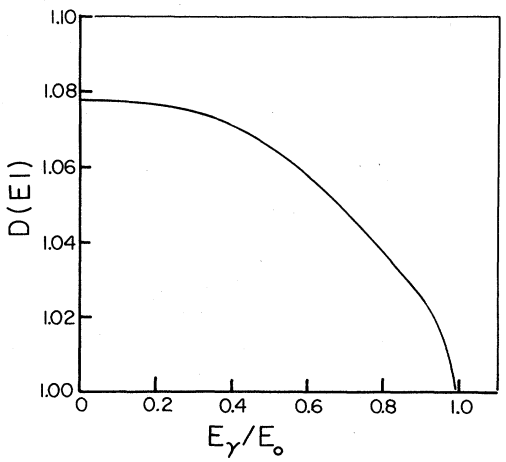

FIG. 6. $E1$ distortion factor defined as the ratio of distorted wave to plane wave virtual photon spectra.

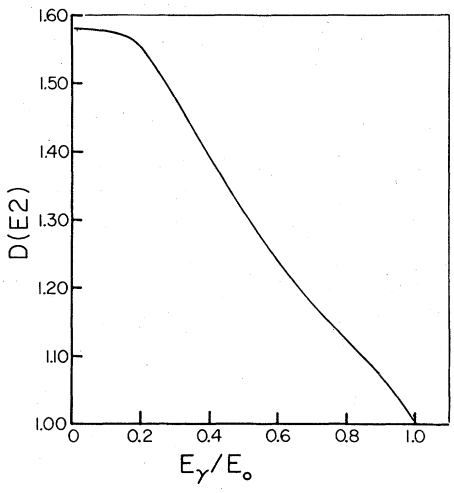

FIG. 7. $E2$ distortion factor.

$\sigma^{E1}_{\gamma,\alpha}(E_\gamma)$ and $\sigma^{E2}_{\gamma,\alpha}(E_\gamma)$. In Fig. 5, the fitted values of the E_1 and $E2$ contribution to $d\sigma/dE$ are shown for one of the isochromats. In Fig. 8 we show σ^{E1} and σ^{E2} for each of the seven isochromats that were measured. The areas were determined and the appropriate sum rules were found. By fitting these data to Lorentzian and Breit-Wigner line shapes the usual resonance parameters can be determined. These results are summarized in Table I. The width and position of the $E2$ resonance are consistent with those found using the angular distribution data. Note that the shape of the $E1$ cross sections in this analysis is primarily determined by the fact that $d^2\sigma/d\Omega dE$ rises, then falls, with the fit determining the relative amounts of $E1$ and $E2$ strength. The $E2$ strength, however, is determined essentially by the fact that the iso-

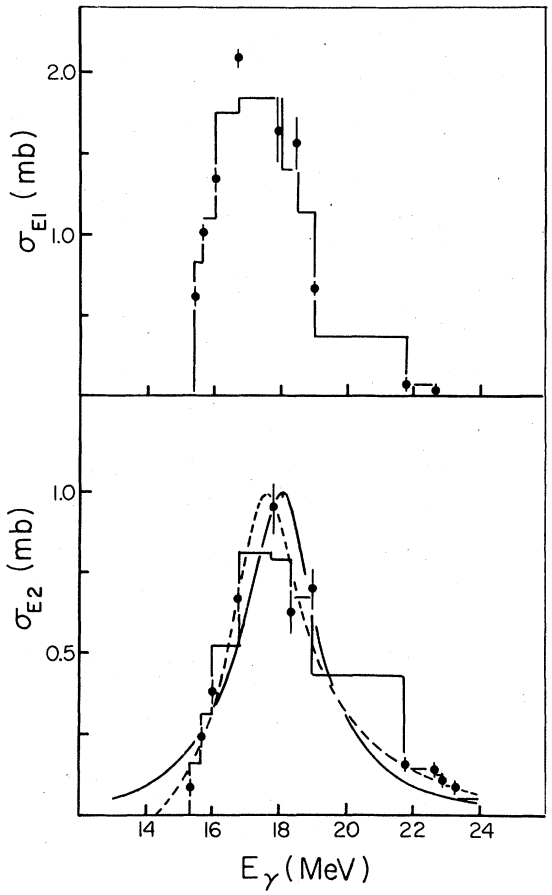

FIG. 8. Total $E1$ and $E2$ cross section determined from the isochromat analysis at seven α energies. The dashed line is the Lorentz line shape fit and the solid line is the Breit-Wigner line shape fit. The resonance parameters are summarized in Table I.

TABLE I. $E2$ integrated cross sections and resonance parameters determined by the isochromat analysis of Sec. IV B.

	Trapezoidal [a] integration	2nd order fit [a] integration	Lorentz line shape	Breit-Wigner line shape
$\int \sigma dE$ (mb MeV)	3.6 ± 0.3	3.8 ± 0.3	3.9 ± 0.1	3.9 ± 0.1
$\int \frac{\sigma dE}{E^2}$ (μb/MeV)	11.0 ± 1.0	11.3 ± 0.9	11.1 ± 1.6	11.1 ± 1.5
% of $E2$ sum rule [b]	28 ± 3	29 ± 2	29 ± 4	29 ± 4
E_R (MeV)			17.9 ± 0.2	18.1 ± 0.2
Γ (MeV)			2.8 ± 0.3	2.9 ± 0.3
σ_0 (mb)			1.00 ± 0.07	1.00 ± 0.06

[a] Reference 13.
[b] We have used the value $0.22Z^2/A^{1/3}$.

chromat rises more rapidly with E_0 near the peak in the measured cross section.

C. Total cross section analysis

The total cross section $\sigma_{e,\alpha}(E_0)$ was found by numerically integrating the cross sections $d^2\sigma/d\Omega dE$ over alpha energy and angle. The angular dependence at $E_0 = 35$ MeV was again assumed to be the same for all incident electron energies. [Taking 4π for the angular integration was found to produce a 4% difference in $\sigma_{e,\alpha}(E_0)$.]

The measured total cross section is shown in Fig. 9. If we analyze these data assuming specific line shapes for σ^{E1} and σ^{E2} in Eq. (2), the total $E1$ and $E2$ cross sections may be determined without an initial assumption with regard to the specific transition taking place, as was done in Sec. IV B. The total cross section was least squares fitted using

$$\sigma_{B\text{-}W} = \sigma_0 \frac{(\Gamma/2)^2}{(E_\gamma - E_R)^2 + (\Gamma/2)^2}$$

and

$$\sigma_L = \sigma_0 \frac{(E\gamma\Gamma)^2}{(E_\gamma^2 - E_R^2)^2 + (E_\gamma\Gamma)^2} .$$

Since the fitting procedure used[10] can minimize χ^2 by varying parallel parameters, the χ^2 parabola is expected to be very shallow. In other words, the particular values of fitted parameters (Γ, E_R, and σ_0) in the above equations that are determined in the fit should not be taken as seriously as the amount of exhaustion that these parameters dictate for the appropriate sum rules.

We have used two methods for determining $\sigma^{(E1)}$ and $\sigma^{(E2)}$ this way. First, we have constrained the fit to give the values $E_R = 17.6$ MeV and $\Gamma = 3.1$ MeV for the $E2$ cross section. These were the parameters that were found from the angular distribution data. Second, we have allowed all the parameters to be fit (six in all) with no constraints. The results are summarized in Table II. As can be seen, the constrained and unconstrained fits give values with respect to the sum rules that are in good agreement.

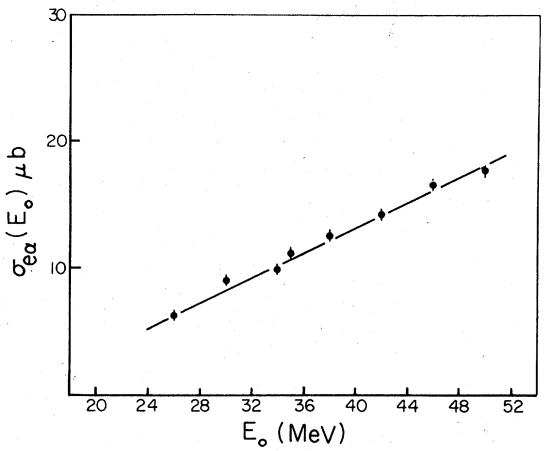

FIG. 9. The total electrodisintegration cross section for the (e,α) channel. The solid line is the result of least square fitting these data with Eq. (1). No appreciable difference was found for Lorentzian and Breit-Wigner line shapes.

Fits to the data assuming that the cross sections were either pure $E1$ or $E2$ resulted in an unsatisfactory χ^2 for either case. Both $E1$ and $E2$ components are required to obtain acceptable values of χ^2. It is also of some comfort that the unconstrained fits give values for E_R and Γ for the $E2$ line shapes that agree reasonably well with the values determined from the angular distribution data. Combining all of these results, we find that the (e,α) cross section exhausts $24 \pm 8\%$ of the isoscalar sum rule for ^{56}Fe which is 39 μb/MeV.[11] The $E1$ integrated cross sections determined by the various analysis procedures are summarized in Table III.

D. Real photon data

To ascertain that monopole transitions were not making a significant contribution to the electrodisintegration cross sections, data were also taken with a thin Ta foil inserted in the beam in front of

TABLE II. $E2$ integrated cross sections and resonance parameters determined by the total cross section analysis of Sec. IV C.

Line shape		σ_0 (mb)	Γ (MeV)	E_R (MeV)	$\int \sigma dE$ (mb MeV)	$\int \sigma dE/E^2$ (mb/MeV)	χ^2	% of $E2$ sum rule
Lorentz	a	0.72 ± 0.02	3.1	17.6	3.04 ± 1.55	8.74 ± 2.82	3.6	22 ± 7
	b	0.99 ± 0.03	2.2 ± 0.2	17.9 ± 0.4	3.14 ± 0.30	9.12 ± 0.42	3.4	23 ± 1
Breit-Wigner	a	0.75 ± 0.02	3.1	17.6	2.99 ± 1.40	8.92 ± 2.84	3.7	23 ± 7
	b	1.00 ± 0.02	2.3 ± 0.1	18.0 ± 0.6	3.13 ± 0.23	9.27 ± 0.15	3.4	24 ± 1

[a] Fit constrained to the $E2$ values of Γ and E_R found from the angular distribution analysis.
[b] Unconstrained fit.

TABLE III. Summary of the $E1$ integrated cross sections for the ^{56}Fe(e,α) reaction and the percentage exhaustion of the sum rule $60NZ/A$.

Analysis		$\int \sigma dE$ (mb MeV)	E_R (MeV)	Γ (MeV)	σ_0 (mb)	% of sum rule
Isochromats		6.41 ± 0.64				0.8 ± 0.1
Lorentz	a	10.51 ± 2.63	16.5 ± 3.1	4.04 ± 0.26	2.19 ± 0.02	1.3 ± 0.3
	b	10.44 ± 0.80	17.0 ± 2.5	4.14 ± 0.30	2.02 ± 0.02	1.2 ± 0.1
Breit-Wigner	a	9.87 ± 3.12	16.7 ± 3.5	4.09 ± 0.3	2.19 ± 0.03	1.2 ± 0.4
	b	9.98 ± 2.19	17.1 ± 2.8	4.25 ± 0.23	2.06 ± 0.02	1.2 ± 0.3

[a] Fit constrained to the $E2$ values of Γ and E_R found from the angular distribution analysis.
[b] Unconstrained fit.

the Fe foil.

The ratio of radiator in to radiator out measurements can be written as

$$\sigma(e+\gamma)/\sigma(e) = 1 + R$$

$$= 1 + \frac{\int_{E_t}^{E_0} \sum_l \sigma_{\gamma,\alpha}^{El}(E_\gamma) N_\gamma(E_0, E_\gamma) \frac{dE_\gamma}{E_\gamma}}{\int_{E_t}^{E_0} \sum_l \sigma_{\gamma,\alpha}^{El}(E_\gamma) N_e^l(E_0, E_\gamma, Z) \frac{dE_\gamma}{E_\gamma}} .$$

If monopole transitions dominate, then no difference between the radiator in and radiator out measurements would be observed since $R \to 0$ in this case. We find that R does not vanish. Furthermore, the quantity $1+R$ serves as a check on the integrated strength for the $E1$ and $E2$ cross sections found in the previous section. Using formula $3BS(e)$ in Koch and Motz[12] to calculate $N_\gamma(E_0, E_\gamma)$, we calculate the expected value of $\sigma(e+\gamma)/\sigma(e)$ and compare it with the experimental ratio.

These results, for three different incident electron energies 40, 45, and 49 MeV, give an average value of $(1+R)_{\text{theor}}/(1+R)_{\text{exp}} = 1.00 \pm 0.02$. We only mean by $(1+R)_{\text{theor}}$ here the value expected using our extracted resonance parameters. We have not considered thick target bremsstrahlung due to the thinness of our radiator. Thus, our analyses would tend to agree more with the Schiff limit given by Hayward[4] for the ^{56}Fe percentage of the $E2$ sum, i.e., $(18 \pm 3)\%$.

V. CONCLUSION

We find that by considering various model-dependent analyses of the ^{56}Fe(e,α) cross section measurements that this channel exhausts a sizable percentage of the $E2$ sum rule $(24 \pm 8\%)$. The angular distribution data which exhibit a definite asymmetry rule out a statistical interpretation as the sole explanation of the data and give reasonable consistency with the parameters determined from the energy-dependent analyses of the (e,α) cross section. Real photodisintegration data were taken that serve as a check on the extracted cross sections and analysis method. The measured ratios of real to virtual processes were consistent with the cross sections extracted from the electrodisintegration data.

ACKNOWLEDGMENTS

This work was partially supported by the National Sciences and Engineering Research Council of Canada. We wish to thank Dr. H. Weller and Dr. E. Hayward for useful discussions and communication of their work. We also thank Mr. L. Custead for assistance with some of the computer programming used in the analyses of the data and Dr. E. Tomusiak for many useful comments.

[1] J. J. Murphy *et al.*, Phys. Rev. C 18, 736 (1978).
[2] J. J. Murphy II, H. J. Gehrhardt, and D. M. Skopik, Nucl. Phys. A277, 69 (1977).
[3] E. Wolynec, W. R. Dodge, and E. Hayward, Phys. Rev. Lett. 42, 27 (1979).
[4] E. Hayward (private communication).
[5] H. R. Weller (private communication).
[6] J. C. McGeorge *et al.*, Nature (London) 280, 724 (1979).
[7] H. Feshbach, in *Nuclear Spectroscopy*, edited by F. Ajzenberg-Selove (Academic, New York, 1960), p. 625.
[8] D. S. Onley and L. E. Wright (private communication).
[9] L. E. Wright (private communication).
[10] K. Fielding, Commun. Assn. Comp. Mach. 13, 509 (1970).
[11] S. S. Hanna, in *Photonuclear Reactions*, edited by S. Costa and C. Schaerf (Springer, New York, 1977), p. 275.
[12] H. W. Koch and J. W. Motz, Rev. Mod. Phys. 31, 920 (1959).
[13] P. R. Bevington, in *Data Reduction and Error Analysis for the Physical Sciences* (McGraw-Hill, Toronto, 1969).